

Experimental measurements of generalized grating images

Daniel Crespo, José Alonso, and Eusebio Bernabeu

The term generalized grating imaging is used to describe the process of image formation of a grating using only another grating as imaging system. The moiré and the Lau effects could be regarded as particular cases of such a process. Here we deal with the less-studied case of images formed at finite distances from the gratings, using an extended monochromatic light source. Some experimental results are shown for the images obtained in this last case, and they are compared with theoretical predictions. © 2002 Optical Society of America

OCIS codes: 050.2770, 050.1960, 070.2590, 070.6760, 110.0110.

1. Introduction

There are several processes for creating images of a grating with only gratings as imaging elements. The best known of these processes is the Talbot effect^{1,2}; self-images of a grating appear at certain distances from it when the grating is illuminated with collimated monochromatic light. In this case the wavelike nature of light, jointly with the periodic structure of the grating, produce its self-images.

There are other cases in which one grating acts as an imaging element for another grating. The Lau effect³ is the best-known example of such a process. In this case two gratings of the same pitch placed parallel to each other and separated by a certain distance are illuminated with an extended monochromatic source, and a pseudoimage of the first grating is formed at infinity. The term pseudoimage is used because the intensity distribution on the observation plane (in this case located at infinity) is a set of well-modulated fringes but with a fringe profile that could be different from that of the first grating. For example, if the first and the second gratings are Ronchi gratings, a set of triangular fringes appears at infinity. The formation of pseudoimages at infinity with

two gratings of the same pitch has also been studied for partially coherent and coherent illumination.⁴ Also, a study of the Lau effect within the theory of partial coherence was presented by Gori.⁵

In the case that the second grating has a slightly different pitch from the first one, pseudoimages of the first grating may appear at a certain number of discrete distances from the second grating.^{6,7}

All these different processes can be regarded within the general formalism of a double diffraction setup illuminated with an extended monochromatic source. Theoretical expressions for the process of generalized grating imaging were recently presented by the current authors.⁸ With the formalism presented, the Talbot and the Lau effects can be regarded as special cases within a more-general formulation. These particular cases have already been thoroughly studied theoretically and are at the basis of many applications.⁹

Our aim in this study is to present some experimental measurements made to validate the theoretical results presented in Ref. 8. This experimental study is centered on the configuration of a double diffraction system in which the pitch of both gratings is different and the formation of pseudoimages occurs at finite distances from the gratings. This is the case that has been less studied in previous literature and for which the results presented in Ref. 8 would be original and therefore would need experimental verification.

Aside from its theoretical interest, the configuration studied in this paper could be interesting for some practical applications, such as optical encoders. For such a configuration it is possible to obtain the maximum modulation of the fringes for a separation

When this research was performed, the authors were with Departamento de Óptica, Universidad Complutense de Madrid, Facultad de Cc. Físicas, Ciudad Universitaria s/n, 28040 Madrid, Spain. D. Crespo (dcrespo@viapostal.com) is now with Via Postal S.A., Torneros 11, 28906 Getafe, Madrid, Spain.

Received 18 September 2000; revised manuscript received 26 June 2001.

0003-6935/02/071223-06\$15.00/0

© 2002 Optical Society of America

between gratings different from 0, which is not the case in the Talbot¹⁰ or the Lau effect.¹¹ This could be used to improve the mechanical tolerances in some applications that make use of a double diffraction system.

In Section 2 we present the theoretical expressions for generalized grating imaging, using a monochromatic extended source. We show how the Talbot and the Lau effects can be obtained as special cases from the general formulation. In Section 3 we present the experimental results obtained for the case in which two Ronchi gratings with different pitch are employed. We analyze these experimental results, comparing them with the theoretical predictions.

2. Theoretical Expressions

The optical system that is used for generalized grating imaging is the one shown in Fig. 1. It consists of a monochromatic extended light source, F , and two periodic gratings, G_1 and G_2 , which can have a different pitch. The distance between the light source and the first grating is z_0 , and the distance between both gratings is z_1 . The size of the light source along the axis perpendicular to the pitch of the gratings is S , with the source size along the gratings' lines not relevant to our discussion. We are studying the light distribution on a plane P located at a distance z_2 from the second grating.

If we consider that G_1 and G_2 are thin gratings, their effect on an incident wave front can be described by a complex periodical transmittance. In this case grating G_1 would be defined by

$$t_1(x) = \sum_n a_n \exp(inq_1x), \quad (1)$$

where $q_1 = 2\pi/p_1$, and p_1 is the pitch of G_1 . In the same manner, G_2 will be given by

$$t_2(x) = \sum_m b_m \exp(imq_2x), \quad (2)$$

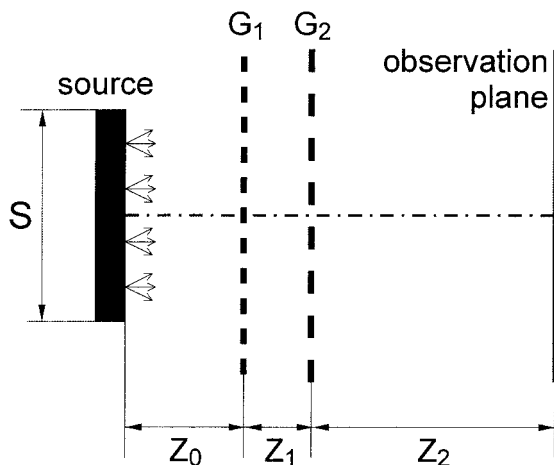


Fig. 1. Schematic view of a double diffraction arrangement with an extended light source.

where $q_2 = 2\pi/p_2$, and p_2 is the pitch of G_2 .

Now we define the following dimensionless quantities,

$$\begin{aligned} R &= \frac{q_2}{q_1}, & Z_0 &= \frac{q_1^2 z_0}{\pi k}, & Z_1 &= \frac{q_1^2 z_1}{\pi k}, \\ Z_2 &= \frac{q_1^2 z_2}{\pi k}, & Z_T &= \frac{q_1^2 z_T}{\pi k}, \end{aligned} \quad (3)$$

where $z_T = z_0 + z_1 + z_2$ and $k = 2\pi/\lambda$. Then, following Ref. 8, the intensity distribution on plane P is given by

$$\begin{aligned} I_S(x) = & \sum_n \sum_{n'} \sum_m \sum_{m'} a_n a_{n'}^* b_m b_{m'}^* \exp \left\{ ix \frac{q_1}{Z_T} [Z_0 \right. \\ & \times (n - n') + R(Z_0 + Z_1)(m - m')] \Big\} \\ & \times \exp \left[i \frac{\pi}{2} \frac{Z_0}{Z_T} (n^2 - n'^2)(Z_1 + Z_2) \right] \\ & \times \exp \left[i \frac{\pi}{2} \frac{Z_0 + Z_1}{Z_T} (m^2 - m'^2) R^2 Z_2 \right] \\ & \times \exp \left[i \pi \frac{Z_0}{Z_T} (nm - n'm') R Z_2 \right] \\ & \times \text{sinc} \left\{ \frac{S}{Z_T} q_1 [(n - n')(Z_1 + Z_2) \right. \\ & \left. + (m - m') R Z_2] \right\}. \end{aligned} \quad (4)$$

We can study the particular case in which both gratings have the same pitch, $R = 1$, and the light from the source is collimated. We can regard the process of collimating a source with a given size as the infinite limit of displacing the source to the left at the same time that we increase the size of the source, such that the quotient $S/z_0 = S'/f$ remains constant during the process, where S' is the actual size of the source placed on the focal plane of the collimating lens with focal length f . Therefore, in expression (4), we can represent a collimated source by making $Z_0 \rightarrow \infty$ and the following substitution: $S/Z_0 = S'/F$, where $F = q_1^2 f / \pi k$, and f is the focal length of the lens used for collimation. In this case the intensity distribution will be

$$\begin{aligned} I_S(x) = & \sum_n \sum_{n'} \sum_m \sum_{m'} a_n a_{n'}^* b_m b_{m'}^* \\ & \times \exp[ixq_1(n - n' + m - m')] \\ & \times \exp \left[i \frac{\pi}{2} (n^2 - n'^2)(Z_1 + Z_2) \right] \\ & \times \exp \left[i \frac{\pi}{2} (m^2 - m'^2) Z_2 \right] \\ & \times \exp[i\pi(nm - n'm') Z_2] \\ & \times \text{sinc}\{S'q_1[(n - n')(Z_1 + Z_2) \\ & + (m - m') Z_2]\}. \end{aligned} \quad (5)$$

This expression corresponds to the case of the standard double diffraction system with coherent, collimated illumination in the infinite fringe configuration.⁹

We can also study the case in which $R = 1$, the source has infinite extent, $S \rightarrow \infty$, and the observation plane is located at the back focal plane of a lens. As previously for the process of collimation, this means that $x/Z_2 = x'/F$ and $Z_2 \rightarrow \infty$, where x' is the actual spatial coordinate on the backfocal plane of the lens, and $F = q_1^2 f / \pi k$ where f is the focal length of the lens. In this case the observed intensity distribution will be

$$I_S(x') = \sum_l \exp\left(-ix' \frac{q_1}{F} Z_1 l\right) \exp\left(-i\frac{\pi}{2} Z_1 l^2\right) \times \sum_n \sum_m a_n a_{n-1}^* b_m b_{m+l}^* \exp(-i\pi Z_1 m l), \quad (6)$$

which corresponds to a set of standard Lau fringes.

These cases, corresponding to the moiré and the Lau effects, are well known and have been studied intensively. We are interested in the case in which both gratings have a different pitch, $R \neq 1$, and the source cannot be considered infinite (partially coherent case). Under these circumstances an infinite family of images will appear at different, finite distances from the second grating. The existence and the location of these images are also well known, for the case in which either incoherent⁶ or partially coherent illumination⁴ is used. But, to our understanding, the exact number of images that will be observable in a system with partially coherent illumination, and the focal depth of those images, has not previously been studied in detail. In a recent study of the present authors,⁸ rigorous conditions were derived for the existence of the pseudoimages and also expressions for the intensity distribution in those zones of the optical axis close to a pseudoimage, which allowed us to determine their focal depth. These conditions can be summarized in the following expressions taken from Ref. 8:

- For a system with given values for S , q_1 , q_2 , Z_0 , and Z_1 , there will be an observable pseudoimage when Z_2 meets the following condition:

$$(Z_1 + Z_2)n_I + RZ_2m_I \approx 0, \quad (7)$$

where n_I and m_I are two integers that must satisfy

$$|n_I| \ll \frac{Sq_1}{\pi Z_T} RZ_2, \quad |m_I| \ll \frac{Sq_1}{\pi Z_T} (Z_1 + Z_2). \quad (8)$$

These two equations determine the location of the observable pseudoimages and also the total number of images that can be observed. In the model previously introduced by Swanson and Leith⁶ for incoherent illumination, there was no restriction on the possible values of n_I and m_I and the pseudoimages had zero focal depth.

- The intensity distribution in the zone of the optical axis close to a pseudoimage can be approximated by the expression

$$I_S(x) \approx I_0 + \sum_{j \neq 0} d_j \exp\left(ix \frac{Z_1}{Z_2} q_1 j n_I\right) \times \text{sinc}\left\{j \frac{Sq_1}{Z_T} [(Z_1 + Z_2)n_I + RZ_2m_I]\right\}, \quad (9)$$

where I_0 is a constant background and

$$d_j = \exp\left(i\frac{\pi}{2} RZ_1 n_I m_I j^2\right) \sum_{n'} a_{n'+jn_I} a_{n'}^* \times \sum_{m'} b_{m'+jm_I} b_{m'}^* \exp(-i\pi RZ_1 n_I m' j). \quad (10)$$

Expression (9) represents a set of fringes of period $p = p_1 Z_2 / Z_1$. From these last two expressions it is possible to derive the focal depth of the pseudoimages.

3. Experimental Results

Our aim in this paper is to show experimental results that confirm the validity of expression (9) and those derived from it. This will be done for the particular case in which both gratings are Ronchi gratings and for the pseudoimages with $(n_I, m_I) = (1, -1)$. Let us define signal modulation as the difference between the maximum and the minimum values of the signal, $M = \max(I_S) - \min(I_S)$. The modulation of the fringes can be approximated in this particular case,⁸ by expression

$$M \approx \left| \frac{1}{\pi^2} \cos\left(\frac{\pi}{2} RZ_1\right) \text{sinc}\left\{\frac{Sq_1}{Z_T} [(Z_1 + Z_2) - RZ_2]\right\} \right|. \quad (11)$$

We use the approximation given by expression (11) as the theoretical prediction for the modulation of the fringes. We prefer this expression because of its simplicity, instead of the exact value of the modulation that would be obtained from Eq. (4) by computing numerically the exact intensity for a complete period of the signal. In the following we test the correctness of the theoretical model by comparing the experimental results with expression (11).

The experimental setup was the one shown in Fig. 1. The observation plane coincides with the array of detectors of a CCD camera with the automatic gain disconnected, and we use the image registered on the camera to calculate the period and the modulation of the observed fringes. The images obtained have low noise levels, and the calculation of the modulation is straightforward, with no need for noise-reduction techniques. In Fig. 2 we show an example of the profile of the registered fringes, compared with the theoretically predicted triangular profile (plus a uniform background). It can be observed that the recorded fringe profile is slightly rounded with respect to the expected triangular profile. There are two factors contributing to this effect. One is the finite

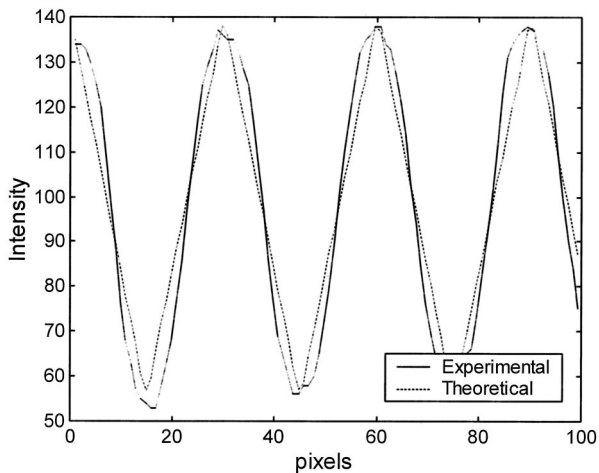


Fig. 2. Profile of the fringes obtained with the CCD camera located on the detection plane. The comparison is shown with a triangular profile.

spectral width of the source, which is approximately $\Delta\lambda \approx 50$ nm. The short temporal coherence will not be important in the self-imaging phenomenon, since we will use gratings with a pitch of $40\text{ }\mu\text{m}$, but each wavelength in the spectra contributes with a fringe pattern of a slightly different period, producing a small smoothing of the fringes but with little effect on the modulation (the effects of wavelength dispersion in double diffraction arrangements, and its dependency on the period of the gratings, can be seen in Ref. 9). Another factor that contributes to the fringe roundness is related to the adjustment of the grating gap. The fringes are triangular when Z_1 meets relation (7). We tuned this parameter in the experimental setup by looking for a maximum of the fringe modulation, but the latter is more insensitive to Z_1 than the shape of the fringes. This means that a small variation of Z_1 changes the fringe profile without appreciably changing the modulation. In any case, this small deviation from the triangular profile in the measurement shown in Fig. 2 does not modify the conclusions presented in this study.

In Fig. 3(a) we show different sets of measurements realized with the experimental arrangement described above. In this case we used gratings of periods, $p_1 = 40\text{ }\mu\text{m}$ and $p_2 = 37\text{ }\mu\text{m}$, which yields a value of $R = 1.08$. As an approximation to a spatially incoherent monochromatic source we used a noncollimated LED whose peak wavelength is $\lambda = 560$ nm. The LED is mounted on a standard metallic package without a collimating lens. The chip is bonded to the bottom plane of a circular tray, which is employed to reflect the light emitted by the vertical sides of the chip, thus increasing the flux emitted in the forward direction. The size of the chip is $347\text{ }\mu\text{m} \times 347\text{ }\mu\text{m}$, and its height is $50\text{ }\mu\text{m}$. The shape of the reflective tray is that of an inverted truncated cone, with an inner diameter of the bottom surface of 0.974 mm and with an outer diameter of 1.480 mm. Although the source structure is complex, the surface of the reflective tray is not polished, so it is a reason-

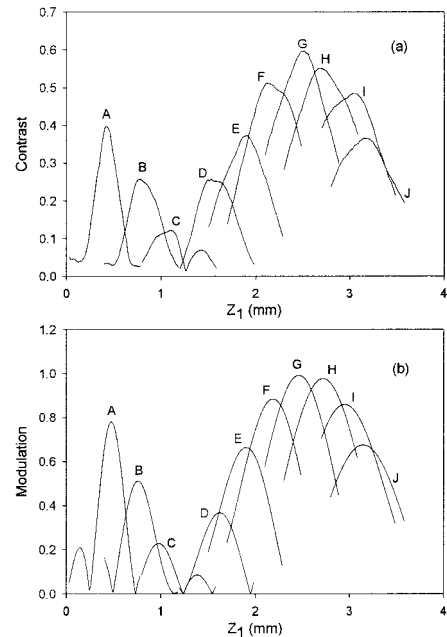


Fig. 3. (a) Experimental measurements of the contrast of the fringes for different values of z_2 . (b) Theoretical predictions for the modulation of the fringes for the same values. Each letter indicates a curve for a different value of z_2 : A, $z_2 = 5$ mm; B, $z_2 = 9$ mm; C, $z_2 = 13$ mm; D, $z_2 = 17$ mm; E, $z_2 = 21$ mm; F, $z_2 = 25$ mm; G, $z_2 = 29$ mm; H, $z_2 = 33$ mm; I, $z_2 = 37$ mm; and J, $z_2 = 41$ mm.

able assumption that the whole structure is equivalent to a diffuse circular source with a size similar to the outer diameter of the reflective tray. In effect, if we make S equal to the size of the LED chip, we do not get good agreement between our model and the experimental results. The agreement improves as we make S closer to the outer diameter of the reflective tray. Indeed, an excellent match (which is presented in Figs. 3–6) is obtained when we make $S = 1.2$ mm. In that sense we may conclude that the structure formed with the chip inside the circular tray with diameter 1.48 mm is equivalent to a spatially incoherent source of size 1.2 mm.

The source was placed approximately 5 mm before the first grating. Each curve on Fig. 3(a) shows the contrast of the fringes formed on the observation plane for a single value of z_2 , and for a certain range of values of z_1 . In Fig. 3(b) we show the theoretical predictions, using expression (11), for the same values of z_1 and z_2 as in Fig. 3(a). It should also be noted that the experimental curves show the measured contrast of the fringes, whereas the theoretical curves show modulation. The contrast of the fringes is defined as

$$V = \frac{\max(I_S) - \min(I_S)}{\max(I_S) + \min(I_S)},$$

so for the calculated expressions, as can be derived from expression (9), modulation is proportional to constant. In our experiment we decided to measure

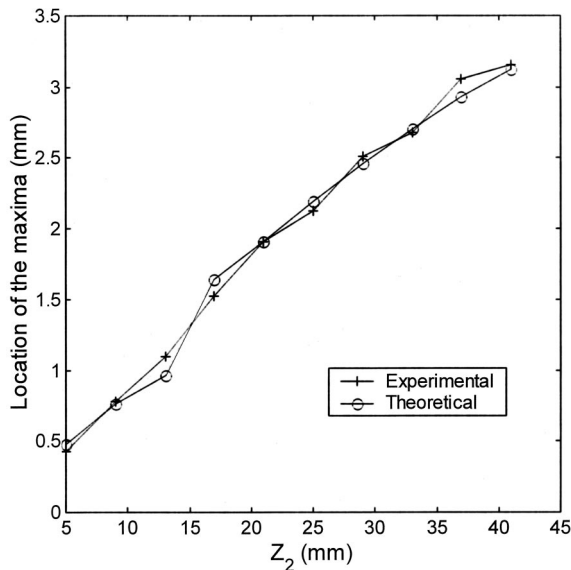


Fig. 4. Theoretical and experimental curves showing the value of Z_1 for which a maximum in the modulation is obtained, as a function of Z_2 .

contrast to make the results independent from possible source fluctuations.

We compare the different curves shown in Fig. 3(a) with those in Fig. 3(b). We study the location of the modulation peaks, their relative heights, and the change of their width for different values of Z_2 , always making comparisons between theory and experiment.

Figure 4 shows the separation between gratings, Z_1 , for which a maximum modulation is obtained, as a function of Z_2 . Two curves are shown, corresponding to the theoretical and the experimental values. As was expected from theory, for larger values of Z_2 ,

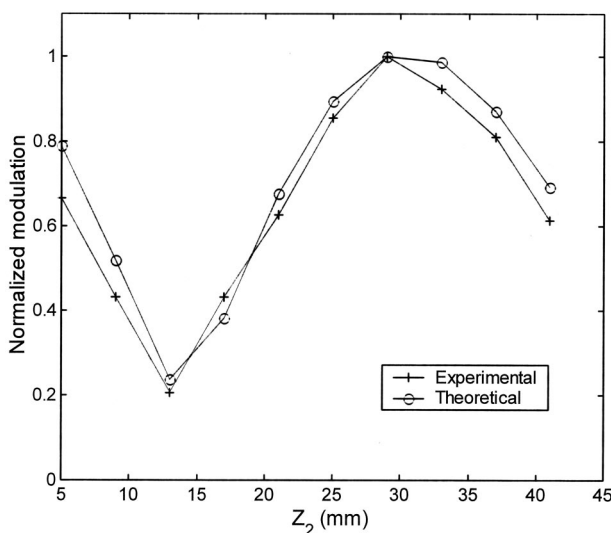


Fig. 5. Comparison between theoretical and experimental curves of the maximum value of the modulation obtained for different values of Z_2 . Both curves are normalized to their respective highest values.

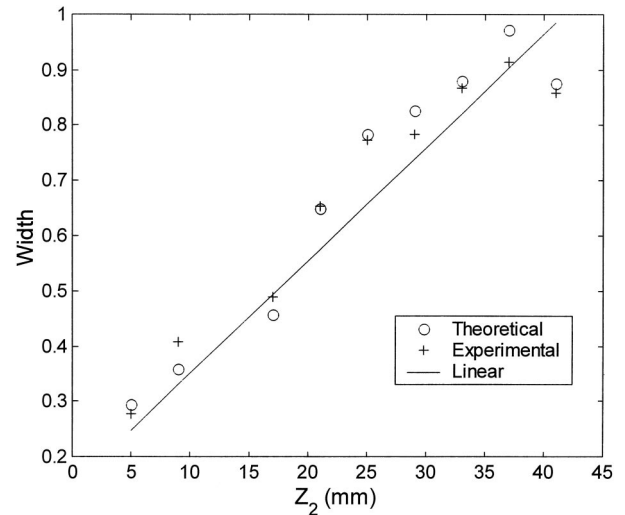


Fig. 6. Curves showing the width at half-maximum of the modulation peaks as a function of Z_2 . The experimental and the theoretical curves are shown, as well as the linear approximation obtained from Eq. (14).

the maximum modulation is obtained for larger values of Z_1 . In fact, from expression (11), a good modulation is obtained only when

$$Z_1 + (1 - R)Z_2 \approx 0, \quad (12)$$

$$RZ_1 \approx 2n \quad (13)$$

at the same time. That is why for certain values of Z_2 it is not possible to obtain a good modulation for any value of Z_1 , as can be seen in curve C in Fig. 3. In Fig. 5 we show the maximum modulation value obtained for any value of Z_1 , as a function of Z_2 . This figure shows a periodic dependence of the maximum attainable modulation with Z_2 . This behavior is the one expected from expression (11).

It is important to study the dependence of the modulation on the grating gap, Z_1 . This is usually the most limiting factor to the mechanical tolerances in a practical application that makes use of a double diffraction system.⁹ In the case that we are studying this stability will be given by the width at half-maximum of the modulation peaks of the curves shown in Fig. 3. At first sight it can be observed that the width of these modulation peaks grows with Z_2 . From expression (11) we can see that an increase in Z_2 (and therefore in Z_T) will make wider the central maximum of

$$f(Z_1) = \text{sinc} \left\{ \frac{Sq_1}{Z_T} [(Z_1 + Z_2) - RZ_2] \right\}, \quad (14)$$

when we consider this last expression as a function of Z_1 . In fact, from this last expression we could consider, as a good approximation, that the width at half-maximum grows proportional to Z_T . In Fig. 6 we show the width at half-maximum of the modulation peaks as a function of Z_2 . We show the values obtained in the experimental and the theoretical

cases, as well as the linear approximation obtained from Eq. (14).

4. Conclusions

We have studied the generalized grating imaging effect in a double diffraction arrangement. We have focused our attention on the case of pseudoimages formed at finite distances from gratings of different pitch when they are illuminated with an extended monochromatic light source. A theoretical study on this effect was recently published by the present authors in Ref. 8. In this study we have presented some experimental measurements of the modulation of the pseudoimages obtained with the mentioned arrangement. The results obtained are in good agreement with the theoretical expressions that were previously obtained.

This study shows, and explains, the depth of focus of the pseudoimages generated at finite distances from a double diffraction arrangement illuminated with monochromatic, partially coherent light. Examples are also shown of the dependency of the modulation of the pseudoimages with the different parameters involved: distance between gratings, location of the detectors, and size of the source.

This study has been supported by the research project from the Comisión Interministerial de Ciencia y Tecnología (CICYT) with reference TAP 98-0862. D. Crespo performed this research while he was in the fellowship program Formación de Profesorado

Universitario (FPU) of the Ministerio de Educación y Ciencia.

References

1. F. Talbot, "Facts relating to optical science. IV," *Philos. Mag.* **9**, 401–407 (1836).
2. E. Bar-Ziv, "Effect of diffraction on the moire image. I. Theory," *J. Opt. Soc. Am.* **2**, 371–379 (1985).
3. E. Lau, "Beugungserscheinungen an Doppellrastern," *Ann. Phys. (Leipzig)* **6**, 417–423 (1948).
4. L. Liu, "Talbot and Lau effects on incident beams of arbitrary wavefront, and their use," *Appl. Opt.* **28**, 4668–4677 (1989).
5. F. Gori, "Lau effect and coherence theory," *Opt. Commun.* **31**, 4–8 (1979).
6. G. J. Swanson and E. N. Leith, "Analysis of the Lau effect and generalized grating imaging," *J. Opt. Soc. Am. A* **2**, 789–793 (1985).
7. E. N. Leith and R. Hershey, "Transfer functions and spatial filtering in grating interferometers," *Appl. Opt.* **24**, 237–239 (1985).
8. D. Crespo, J. Alonso, and E. Bernabeu, "Generalized grating imaging using a monochromatic extended light source," *J. Opt. Soc. Am. A* **17**, 1231–1240 (2000).
9. K. Paturski, "Influence of the type of illumination and separation of gratings on the intensity distribution in moiré fringes," in *Handbook of the Moiré Fringe Technique* (Elsevier, Amsterdam, 1993), Chap. 4, pp. 69–98.
10. E. Keren and O. Kafri, "Diffraction effects in moiré deflectometry," *J. Opt. Soc. Am. A* **2**, 111–120 (1985).
11. D. Crespo, J. Alonso, T. Morlanes, and E. Bernabeu, "Optical encoder based on the Lau effect," *Opt. Eng.* **39**, 817–824 (2000).